18th International Conference on Information Fusion
Washington, DC - July 6-9, 2015

Data Fusion with ML-PMHT for Very Low SNR Track Detection in an OTHR

Kevin Romeo, Yaakov Bar-Shalom, and Peter Willett
Dept. of Electrical and Computer Engineering
University of Connecticut, Storrs, CT 06269-4157
{romeo, ybs, willett}@engr.uconn.edu

***Abstract*—The Maximum Likelihood Probabilistic Multi-Hypothesis Tracker (ML-PMHT), which is a Deep Target Extractor (DTE), is formulated for and applied to Over-The-Horizon radar (OTHR) scenarios: a constant altitude target and a constant vertical acceleration target. In an OTHR scenario there are two ionosphere layers assumed here to be acting as reflectors of the EM waves and each scan can contain multiple measurements (up to four) originating from each target; each of these target-originated measurements takes one of four possible round-trip paths. The multipath ML-PMHT likelihood ratio models this uncertainty in the measurement path which then allows the fusion of multipath data in the presence of false measurements. This tracker is shown to have high track accuracy in these very low SNR OTHR scenarios.**

I. Introduction

Over-the-horizon radar (OTHR) has the ability to detect targets beyond the horizon using signals refracted through the ionosphere. The signal from the radar may propagate through multiple paths due to the nature of the ionosphere. This can result in several target originated detections in a single frame. The path that corresponds to each target detection is unknown, which creates an ambiguity between detections and paths. Many measurements due to false detections can also occur in OTHR scenarios, further adding to the difficulty of the problem.

Many different approaches have been applied to OTHR tracking. These include the multipath probabilistic data association (MPDA) algorithm [11] and the multiple detection multiple hypothesis tracker (MD-MHT) [14]. The MD-MHT approach uses an extended multi-frame assignment method to solve the data association problem between measurements and measurement paths. Other approaches that can be used are the Probabilistic Data Association Filter (PDAF) [6–8] and the Probabilistic Multiple Hypothesis Tracker (PMHT) [8]. The Multiple Model Unified PDAF (MM-UPDAF) [6] is an extension of the PDAF which is designed to process numerous, non-uniform clutter regions. The lowest SNR considered in [11] and [14] is around 10 dB, with an ionosphere model similar to what we use in our simulations. With a very low observable (VLO) target SNR of 4dB, we demonstrate that our algorithm produces a high track detection probability and accuracy for the considered scenarios, i.e., the ML-PMHT is a Deep Target Extractor (DTE) — it can extract targets buried deeply in noise.

The Maximum Likelihood Probabilistic Multi-Hypothesis Tracker (ML-PMHT) has previously been formulated for single and multitarget [17, 18] scenarios. It has been shown to perform well even with very low target SNR. In [12] we presented an extension to its formulation that allows for multiple possible propagation paths and applied it to a scenario with a surface target. Here we apply the multipath formulation of the ML-PMHT to two OTHR scenarios where the altitude of the target is unknown. Unlike the MD-MHT, no data association is required. The ML-PMHT considers simultaneously all the measurements without knowing their origins or propagation paths and, remarkably, has *linear complexity in the number of measurements*. The ML-PMHT performs fusion of the multipath data in the presence of false measurements.

Section II briefly describes the ML-PMHT for a single target case and the extension to allow for multiple paths. Section III presents the OTHR model used for simulations. Section IV discusses the performance of the ML-PMHT from Monte Carlo testing.

II. ML-PMHT

A. Single Target ML-PMHT

The ML-PMHT log-likelihood ratio (LLR) for the motion parameter of a single target was developed in [17] and is given by

$$\Lambda(\mathbf{x}; Z) \triangleq \ln\left\{\frac{p(Z|\mathbf{x})}{p(Z|\text{all false})}\right\} \tag{1}$$

$$= \sum_{i=1}^{N_w}\sum_{j=1}^{m_i} \ln\left\{\pi_0 + \pi_1 V p[\mathbf{z}_j(i)|\mathbf{x}(i)]\rho_j(i)\right\} \tag{2}$$

Proc. 18th International Conference on Information Fusion (Fusion 2015), Washington, DC, July 2015.
Supported by ARO W991NF-10-1-0369.

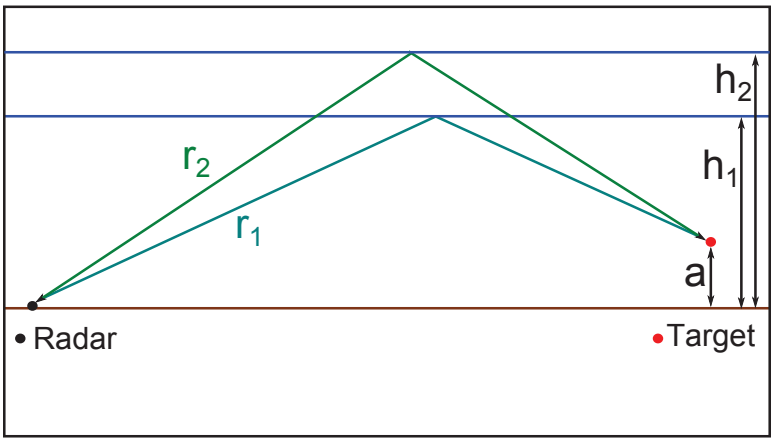

Fig. 1: An illustration of the geometry used to derive the equations for the measurements.

with

$$Z \triangleq \{\{\mathbf{z}_j(i)\}_{j=1}^{m_i}\}_{i=1}^{N_w} \tag{3}$$

Here N_w is the number of scans in the batch (the window length), and m_i is the number of measurements in the i^{th} scan (frame). The parameter $\mathbf{x}$ determines the target state $\mathbf{x}(i)$ in a deterministic way (we use a constant velocity model[1]). The prior probabilities that a measurement occurred due to clutter or due to a target are given by π_0 and π_1, respectively. These values are related to the probability of detection, P_D, and the probability of false alarm in a resolution cell, P_{FA}. The volume of the search region is V and a measurement, if false, has pdf V^{-1}. The j^{th} measurement in the i^{th} scan is $\mathbf{z}_j(i)$ and its associated amplitude likelihood ratio is $\rho_j(i)$. Finally, $p[\mathbf{z}_j(i)|\mathbf{x}(i)]$ is Gaussian with mean determined by the target state parametrization $\mathbf{x}(i)$. The amplitude likelihood ratio serves as a feature discriminant between the target-originated measurements and the false ones due to spurious detections.

The pdfs $p[Z(i)|\mathbf{x}(i)]$ (target present hypothesis) and $p[Z(i)|\text{all false}]$ (target absent hypothesis) are derived using the ML-PMHT DTE assumptions [17]:

- There is a single target with known probability of detection.
- Any number of measurements in a scan can be assigned to the target.
- The motion of the target is deterministic.
- False detections are uniformly distributed.
- The number of false detections is Poisson distributed with known density.
- Amplitudes of target and false detections are Rayleigh distributed with known distribution.
- Target measurements are corrupted with zero-mean Gaussian noise.
- Measurements at different times, conditioned on the parameterized state, are independent.

[1] Alternatively a deterministic motion model in a known gravitational field can be used [4].

These pdfs are then given by

$$p[Z(i)|\mathbf{x}(i)] = \prod_{j=1}^{m_i}\left\{\frac{\pi_0}{V}p_0^\tau[\alpha_j(i)] + \pi_1 p[\mathbf{z}_j(i)|\mathbf{x}(i)]p_1^\tau[\alpha_j(i)]\right\} \tag{4}$$

$$p[Z(i)|\text{all false}] = \prod_{j=1}^{m_i}\frac{1}{V}p_0^\tau[\alpha_j(i)] \tag{5}$$

where $p_0^\tau[\alpha_j(i)]$ and $p_1^\tau[\alpha_j(i)]$ are the pdfs of a false alarm and target measurement amplitude conditioned on exceeding the threshold τ, respectively.

B. The Multipath ML-PMHT Log-Likelihood Ratio for OTHR

The generalized ML-PMHT that allows multiple propagation paths is given by

$$\Lambda(\mathbf{x};Z) = \sum_{i=1}^{N_w}\sum_{j=1}^{m_i}\ln\left\{\pi_0 + \pi_1 V\rho_j(i)\sum_{\ell=1}^{n_p}p[\mathbf{z}_j(i)|\mathbf{x}(i),\ell]P[\ell]\right\} \tag{6}$$

where ℓ is used to denote which path the signal took, $P[\ell]$ is the probability of path ℓ being taken, and n_p is the total number of possible paths. The mean of the Gaussian $p[\mathbf{z}_j(i)|\mathbf{x}(i),\ell]$ is $f_\ell(\mathbf{x}(i))$, where f_ℓ is the function that transforms the target state $\mathbf{x}(i)$ into the measurement space via path ℓ. Note that we have assumed that $\rho_j(i)$ is the same for each path ℓ.

$$r_1 \triangleq -(h_1(a^2 - 4ah_1 + 4h_1^2 + s_r^2 - 2s_r s_t + s_t^2)^{1/2})/(a - 2h_1) + ((a - h_1)(a^2 - 4ah_1 + 4h_1^2 + s_r^2 - 2s_r s_t + s_t^2)^{1/2})/(a - 2h_1) \quad (14)$$

$$\dot{r}_1 \triangleq \frac{\partial r_1}{\partial s_t}\frac{\partial s_t}{\partial t} = \dot{s_t}(h_1(2s_r - 2s_t))/(2(a - 2h_1)(a^2 - 4ah_1 + 4h_1^2 + s_r^2 - 2s_r s_t + s_t^2)^{1/2}) - \dot{s_t}((2s_r - 2s_t)(a - h_1))/(2(a - 2h_2)(a^2 - 4ah_1 + 4h_1^2 + s_r^2 - 2s_r s_t + s_t^2)^{1/2}) \quad (15)$$

	Constant Altitude Scenario	Constant Acceleration Scenario
Resolution cell size	15 km x 30 m/s	15 km x 30 m/s
Search region size	300 km x 600 m/s x 10 km	300 km x 100 m/s^2
Number of cells	400	400
Amplitude detection threshold τ	2.5	2
P_D for each path	0.41	0.56
P_{FA} in a cell	0.044	0.14
Expected number of false alarms per scan	18	54
π_0	0.9147	0.9599

TABLE II: Scenario parameters used in the constant altitude and constant acceleration simulations.

N_w	10
Time between scans	1 s
σ_r	300 m
$\sigma_{\dot{r}}$	5 m/s
SNR in a cell	$\mathbf{2.5 = 4\,dB}$
Ionosphere lower layer height	100 km
Ionosphere upper layer height	200 km
$P[\ell]$ for all ℓ	0.25

TABLE I: Scenario parameters used in the both the constant altitude and constant acceleration simulations.

III. OTHR Model

We investigate two two-dimensional OTHR scenarios which assume the target to be in a plane. We use a two-layer reflection model for the ionosphere.[2] In this model the signal may reflect from either layer of the ionosphere resulting in multiple (up to four) round-trip propagation paths. The radar measures slant range, slant range rate, and amplitude.

A. Measurement Amplitudes

We model the amplitudes of the measurements according to a Swerling I model [4]. The amplitude is Rayleigh distributed with pdfs

$$p_0(\alpha) = ae^{-\frac{\alpha^2}{2}} \qquad \alpha \geq 0 \quad (7)$$

$$p_1(\alpha) = \frac{\alpha}{1+d}e^{-\frac{\alpha^2}{2(1+d)}} \qquad \alpha \geq 0 \quad (8)$$

for the noise only and target, respectively. Here d is the expected SNR of the target in a resolution cell. For a chosen threshold τ we have

$$P_D = \int_\tau^\infty p_1(\alpha)d\alpha \quad (9)$$

$$P_{FA} = \int_\tau^\infty p_0(\alpha)d\alpha \quad (10)$$

The pdfs of the amplitude of a measurement given that it has exceeded the threshold τ are

$$p_0^\tau(\alpha) = \frac{1}{P_{FA}}p_0(\alpha) \qquad \alpha \geq \tau \quad (11)$$

$$p_1^\tau(\alpha) = \frac{1}{P_D}p_1(\alpha) \qquad \alpha \geq \tau \quad (12)$$

and the amplitude likelihood ratio is then

$$\rho_j(i) = \frac{p_1^\tau[\alpha_j(i)]}{p_0^\tau[\alpha_j(i)]} \quad (13)$$

B. Measurements

The OTHR measures both position and velocity of the target via slant range and slant range rate measurements. For the constant altitude scenario (the constant acceleration scenario has a different slant range rate equation, but can be derived similarly) the equations of the measurements, given the signal reflected off the lower layer in both directions, are given below. Using the definitions in equations (14) and (15), one has

$$z_{r_1} = 2r_1 + w_{r_1} \quad (16)$$

$$z_{\dot{r}_1} = 2\dot{r}_1 + w_{\dot{r}_1} \quad (17)$$

Here h_1 is the height of the lower ionosphere layer. The locations of the radar and target are given by s_r and s_t, respectively. The altitude of the target is a. An illustration of the geometry of this problem is shown in Fig. 1. The velocity of the target is $\dot{s}_t$. The noise terms, w_{r_1} and $w_{\dot{r}_1}$, are zero-mean, Gaussian, independent of

[2]The actual paths are subject to refraction, which requires numerical algorithms for ray tracing. The reflection model used here is a simplified one, which, however, captures the essence of the OTHR.

each other, and with variances σ_r and $\sigma_{\dot{r}}$, respectively. We assume, for simplicity, the same noise variances on all paths.

Given that the signal reflected off the upper layer only (with height h_2), we can find similar equations for r_2, $\dot{r}_2$, z_{r_2}, and $z_{\dot{r}_2}$, with noises w_{r_2} and $w_{\dot{r}_2}$. The equations for the measurements resulting from the remaining two paths, where the signal reflects off of alternate layers, can then be expressed as

$$z_{r_3} = r_1 + r_2 + w_{r_3} \tag{18}$$

$$z_{\dot{r}_3} = \dot{r}_1 + \dot{r}_2 + w_{\dot{r}_3} \tag{19}$$

$$z_{r_4} = r_1 + r_2 + w_{r_4} \tag{20}$$

$$z_{\dot{r}_4} = \dot{r}_1 + \dot{r}_2 + w_{\dot{r}_4} \tag{21}$$

C. Constant Altitude Simulation Parameters

We simulated a target with an initial position of 2150 km away from the radar, an altitude of 6 km, and moving with a constant speed of 200 m/s towards the radar. The other values used in the constant altitude simulations are given in Tables I and II. False measurements are generated uniformly in the measurement space. Note that, due to the very low SNR in a cell, P_D is 0.41 and the low threshold leads to 18 false measurements per scan.

D. Constant Acceleration Simulation Parameters

We also simulated a target 2150 km away from the radar that is initially stationary on the surface. It is has a constant vertical acceleration of 40 m/s^2. The other values used in the constant acceleration simulation are given in Tables I and II. The very low SNR in a cell now leads to 54 false measurements per scan. Figures 2 shows the measurements used (after amplitude thresholding) in one run of the tracker from this scenario. Note that there are usually zero to three target originated measurements in each scan (rarely all four) and the large number of false measurements, which, however, can be successfully handled by the multipath ML-PMHT track detector. Figure 3 shows the amplitude of the measurement in each radar cell before applying the detection threshold. Note the large number of measurements exceeding the threshold, and that it is not readily apparent which are target-originated.

IV. Performance of the Track Detector

A. Constant Altitude Results

The log-likelihood ratio of the ML-PMHT for a single run is shown in Figures 4 and 5 for the constant altitude scenario. There are five peaks resulting from path ambiguity. The central peak (the correct one), however, is easily distinguishable from the side peaks and from any peak occurring due to clutter.

We use a simple grid search with 1 km spacing in range, 100 m/s spacing in velocity, and 0.5 km spacing in altitude to get into the neighborhood of the global maximum of (6). For simplicity, no target feature was used. We then run a local optimization routine from MATLAB using an interior-point algorithm on the highest valued point from the grid search to produce the final state estimate. From 1000 Monte Carlo runs the RMS errors for position, velocity, and altitude at the end of the batch were 172 m, 0.65 m/s, and 1.2 km, respectively. There were no false tracks or missed tracks.

B. Constant Acceleration Results

Figure 6 shows the LLR for the constant acceleration scenario. We use the same search method as in the constant altitude scenario. From 1000 Monte Carlo runs the RMSE values were 33 m in position and 0.03 m/s^2 in acceleration. As in the other scenario, there were no false tracks or missed tracks.

V. Conclusions

We have developed an extension to the single target ML-PMHT DTE (Deep Target Extractor) to allow for the fusion of data from multiple signal propagation paths. We applied this algorithm to two OTHR scenarios: a constant altitude target and a constant acceleration vertical launch target. We showed that, with low target SNR even down to 4 dB post-signal processing, the fusion ML-PMHT has excellent track detection and accuracy in such a scenario. Consequently, the ML-PMHT holds great promise as a DTE in increasing the sensitivity and robustness of the next generation OTHR. Future work would include using a spherical Earth and a more accurate ionosphere model.

References

[1] R. H. Anderson and J. L. Krolik, "Multipath track association for over-the-horizon radar using a bootstrapped statistical ionospheric model," *Conference Record of the Thirty-Third Asilomar Conference on Signals, Systems, and Computers*, vol. 1, pp. 8–14, 1999.

[2] R. H. Anderson and J. L. Krolik, "Track association for over-the-horizon radar with a statistical ionospheric model," *IEEE Transactions on Signal Processing*, vol.50, no.11, pp.2632–2643, 2002.

[3] Y. Bar-Shalom, X.-R. Li, and T. Kirubarajan, *Estimation with Applications to Tracking and Navigation*. New York: Wiley, 2001.

[4] Y. Bar-Shalom, P. K. Willett, and X. Tian, *Tracking and Data Fusion*. Storrs, CT: YBS Publishing, 2011.

[5] W. R. Blanding, P. K. Willett, and Y. Bar-Shalom, "Offline and Real-Time Methods for ML-PDA Track Validation," *IEEE Transactions on Signal Processing*, vol. 55, no. 5, pp. 1994–2006, May 2007.

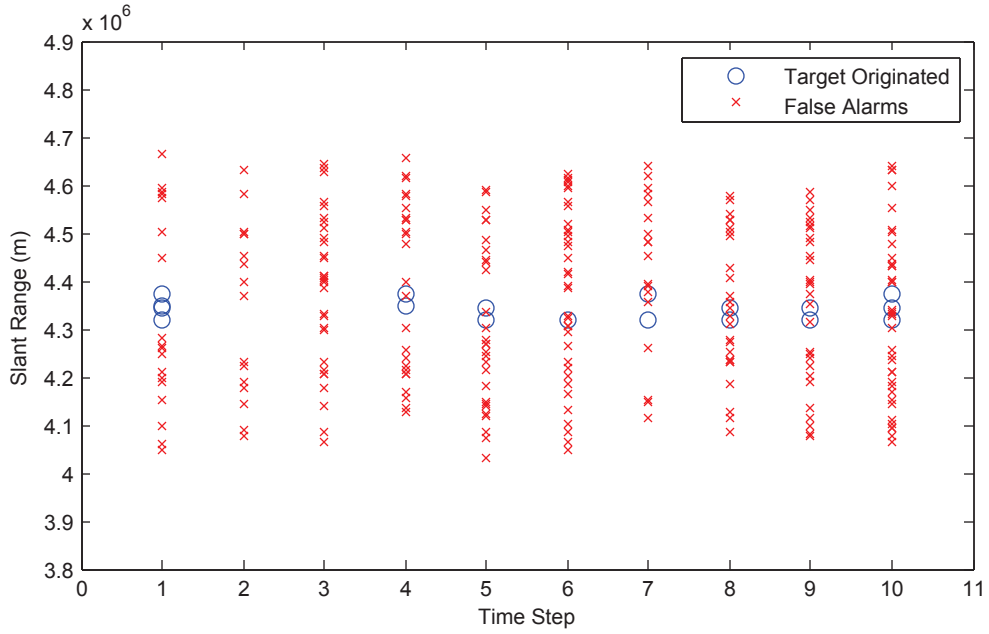

Fig. 2: Slant range measurements in one batch in the constant acceleration scenario (4dB post-signal processing SNR). It is not known to the track extractor which measurements are target-originated.

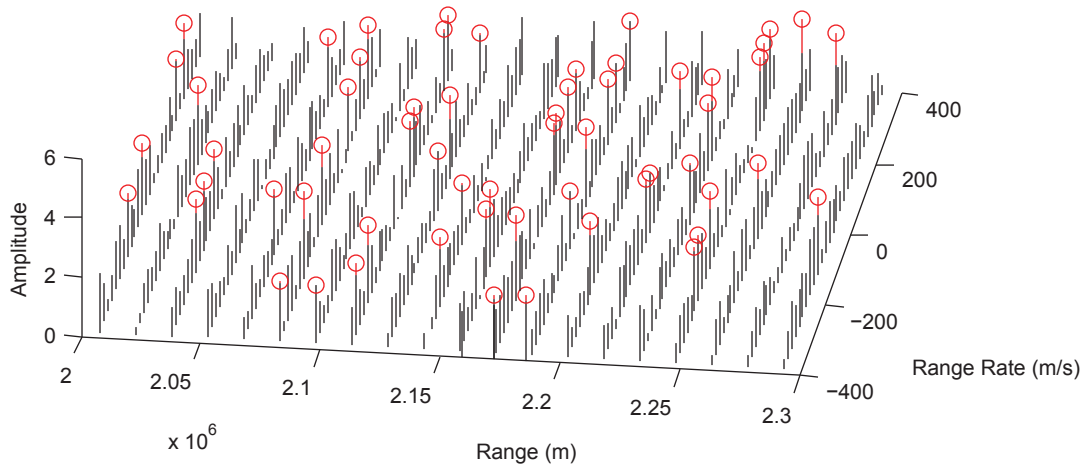

Fig. 3: The amplitude of the measurement in each radar cell, drawn from the center of each cell. Black lines indicate the portion of amplitude below the detection threshold, while red lines (marked with a circle at the top) indicate the portion above the detection threshold. Lines with red are the measurements used by the DTE. Note the large number of measurements exceeding the threshold, and that it is not readily apparent which are target-originated.

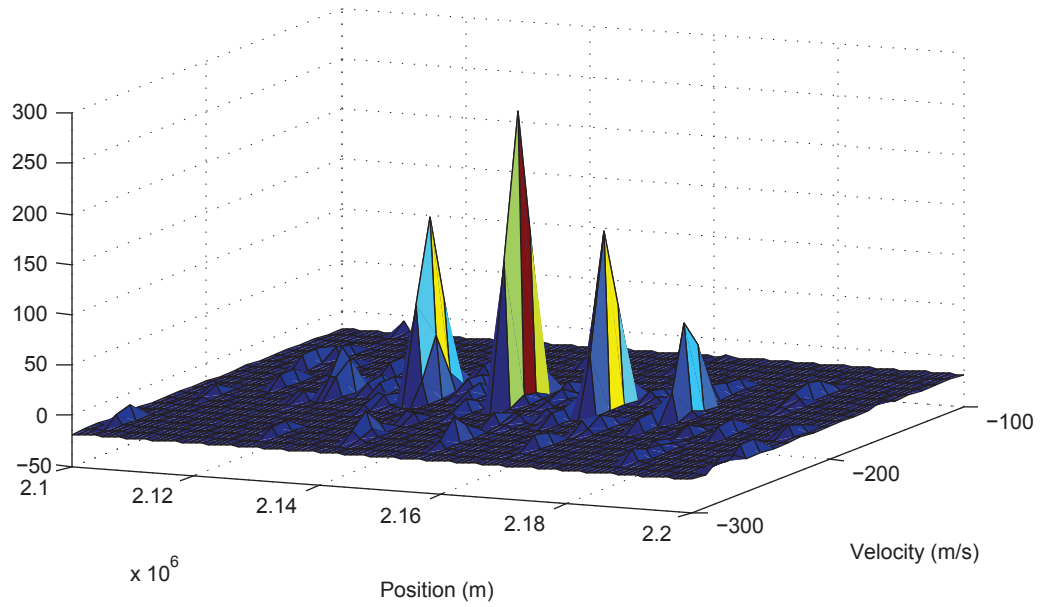

Fig. 4: The log-likelihood ratio at the true value for altitude from the constant altitude scenario.

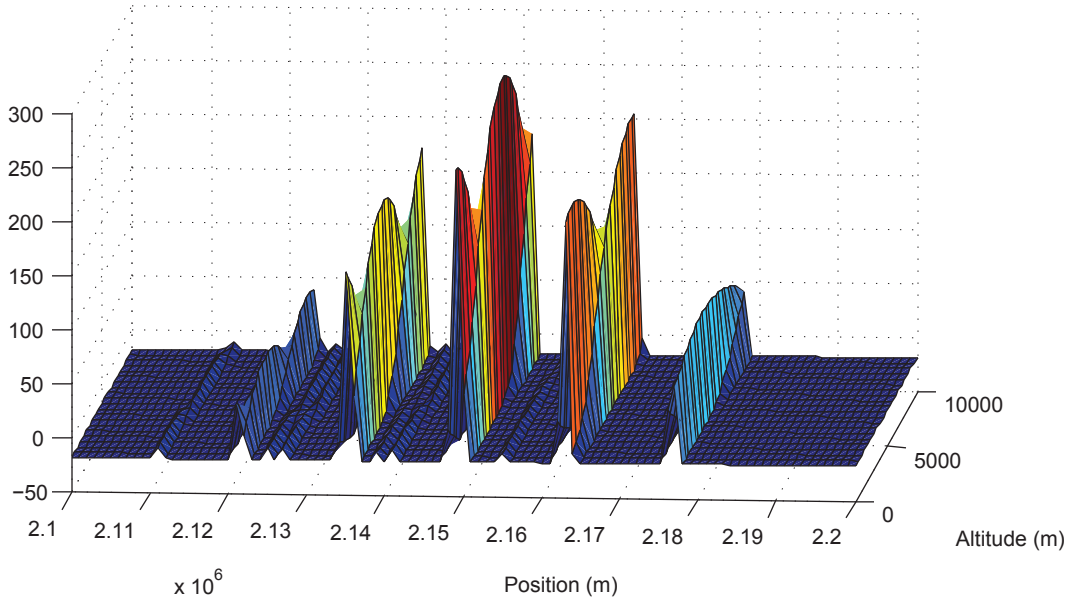

Fig. 5: The log-likelihood ratio at the true value for velocity from the constant altitude scenario.

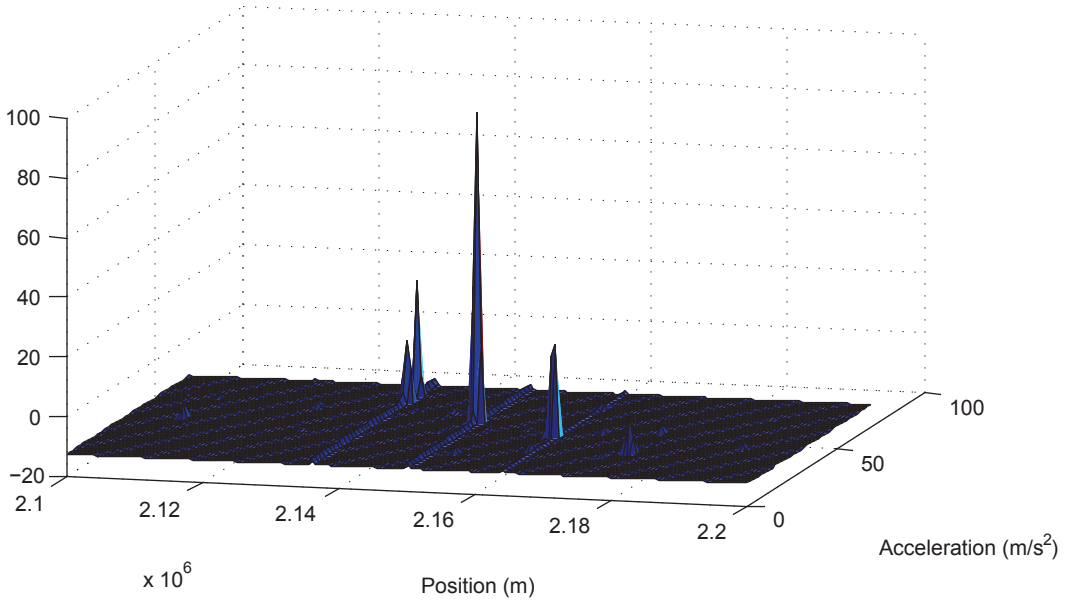

Fig. 6: The log-likelihood ratio from the constant acceleration scenario.

[6] S. B. Colegrove and S. J. Davey, "PDAF with multiple clutter regions and target models," *IEEE Transactions on Aerospace and Electronic Systems*, vol. 39, no. 1, pp. 110–124, January 2003.

[7] S. B. Colegrove and S. J. Davey, "The probabilistic data association filter with multiple nonuniform clutter regions," *The Record of the IEEE 2000 International Radar Conference, 2000*, pp. 65–70, 2000.

[8] S. B. Colegrove, S. J. Davey, and B. Cheung, "PDAF versus PMHT performance on OTHR data," *Proceedings of the International Radar Conference, 2003*, pp. 560–565, September 2003.

[9] S. V. Fridman and L. J. Nickisch, "SIFTER: Signal inversion for target extraction and registration," *Radio Science*, vol. 39, no. 1, 2004.

[10] H. Lan, Y. Liang, Q. Pan, F. Yang, and C. Guan, "An EM Algorithm for Multipath State Estimation in OTHR Target Tracking," *IEEE Transactions on Signal Processing*, vol. 62, no. 11, pp. 2814–2826, 2014.

[11] G. W. Pulford and R. J. Evans, "A Multipath Data Association Tracker for Over-the-Horizon Radar," *IEEE Transactions on Aerospace and Electronic Systems*, vol. 34, no. 4, pp. 1165–1183, October 1998.

[12] K. Romeo, Y. Bar-Shalom, and P. Willett, "Fusion of Multipath Data with ML-PMHT for Very Low SNR Track Detection in an OTHR," submitted to *Journal of Advances in Information Fusion*, 2015.

[13] M. G. Rutten and D. J. Percival, "Comparison of track fusion with measurement fusion for multipath OTHR surveillance," *Proceedings of the 4th International Conference on Information Fusion*, 2001.

[14] T. Sathyan, T.-J. Chin, S. Arulampalam, and D. Suter, "A Multiple Hypothesis Tracker for Multitarget Tracking With Multiple Simultaneous Measurements," *IEEE Journal of Selected Topics in Signal Processing*, vol. 7, no. 3, pp. 448–460, June 2013.

[15] S. Schoenecker, P. Willett and Y. Bar-Shalom, "Extreme-Value Analysis for ML-PMHT, Part 1: Target Trackability", *IEEE Trans. Aerosp. Electronic Systems*, 2014 (in print).

[16] S. Schoenecker, P. Willett and Y. Bar-Shalom, "Extreme-Value Analysis for ML-PMHT, Part 2: False Track Probability", *IEEE Trans. Aerosp. Electronic Systems*, 2014 (in print).

[17] S. Schoenecker, P. Willett, and Y. Bar-Shalom, "Maximum Likelihood Probabilistic Multi-Hypothesis Tracker Applied to Multistatic Sonar Data Sets," *Proc. SPIE Conf. on Signal Processing, Sensor Fusion, and Target Recognition*, Orlando, FL, 2011.

[18] S. Schoenecker, P. Willett, and Y. Bar-Shalom, "ML-PDA and ML-PMHT: Comparing Multistatic Sonar Trackers for VLO Targets Using a New Multitarget Implementation," *IEEE Journal of Oceanic Engineering*, 2014 (in print).